molecular oral microbiology

molecular oral microbiology

D-Alanine metabolism is essential for growth and biofilm formation of *Streptococcus mutans*

W. Qiu[1,*], X. Zheng[1,2,*], Y. Wei[1,2], X. Zhou[1,2], K. Zhang[1], S. Wang[1,2], L. Cheng[1,2], Y. Li[1], B. Ren[1], X. Xu[1,2], Y. Li[1] and M. Li[1]

1 State Key Laboratory of Oral Diseases, Sichuan University, Chengdu, China
2 Department of Operative Dentistry and Endodontics, West China Hospital of Stomatology, Sichuan University, Chengdu, China

Correspondence: Mingyun Li, State Key Laboratory of Oral Diseases, West China Hospital of Stomatology, Sichuan University, No. 14 Renmin South Road, Chengdu 610041, China Tel.: 86-28-85501232; fax: 86-28-85501436; E-mail: limingyun@scu.edu.cn
*These two authors contributed equally to this study.

Keywords: adhesion; D-alanine metabolism; antimicrobial; biofilms; dental caries; *Streptococcus mutans*
Accepted 28 October 2015
DOI: 10.1111/omi.12146

SUMMARY

Part of the D-alanine (D-Ala) metabolic pathway in bacteria involves the conversion of L-alanine to D-Ala by alanine racemase and the formation of D-alanyl–D-alanine by D-alanine–D-alanine ligase, the product of which is involved in cell wall peptidoglycan synthesis. At present, drugs that target the metabolic pathway of D-Ala are already in clinical use – e.g. D-cycloserine (DCS) is used as an antibiotic against *Mycobacterium tuberculosis*. *Streptococcus mutans* is the main cariogenic bacterium in the oral cavity. Its D-Ala metabolism-associated enzymes alanine racemase and D-alanine–D-alanine ligase are encoded by the genes *smu.1834* and *smu.599*, respectively, which may be potential targets for inhibitors. In this study, the addition of DCS blocked the D-Ala metabolic pathway in *S. mutans*, leading to bacterial cell wall defects, significant inhibition of bacterial growth and biofilm formation, and reductions in extracellular polysaccharide production and bacterial adhesion. However, the exogenous addition of D-Ala could reverse the inhibitory effect of DCS. Through the means of drug regulation, our study demonstrated, for the first time, the importance of D-Ala metabolism in the survival and biofilm formation of *S. mutans*. If the growth of *S. mutans* can be specifically inhibited by designing drugs that target D-Ala metabolism, then this may serve as a potential new treatment for dental caries.

INTRODUCTION

D-Alanine (D-Ala) metabolism, an important step in the synthesis of cell wall peptidoglycan in prokaryotes, involves two main reactions: the conversion of L-alanine to D-Ala by alanine racemase (Alr, EC 5.1.1.1) (Hols *et al.*, 1997; Chacon *et al.*, 2009), and the formation of D-alanyl–D-alanine dipeptide from D-Ala by D-alanine–D-alanine ligase (Ddl, EC 6.3.2.4) (Mullins *et al.*, 1990; Batson *et al.*, 2010). The C-terminal D-Ala of the D-alanyl–D-alanine dipeptide, which is also located at the C-terminus of the peptidoglycan precursor uridine diphosphate-*N*-acetylmuramyl-pentapeptide, is directly involved in the cross-linking of adjacent peptidoglycan chains in the bacterial cell wall (Neuhaus, 1962; Lu *et al.*, 2007). Therefore, the inhibition of enzymes involved in the D-Ala metabolic pathway can inhibit the biosynthesis of peptidoglycan precursors, which in turn affects the formation of bacterial cell wall and prevents bacterial growth. As a cyclic analogue of D-Ala, D-cycloserine (DCS) is a competitive inhibitor of alanine racemase and D-alanyl–D-alanine ligase (Halouska *et al.*, 2014). Currently, DCS is used as a second-line anti-tuberculosis drug.

Despite the presence of hundreds of indigenous oral flora, dental caries result from the overgrowth of a handful of cariogenic pathogens (Takahashi & Nyvad, 2011;). Evidence suggests that *Streptococcus mutans* is the principal etiological agent for dental caries in most cases (Beighton, 2005; Corby *et al*., 2005), which produces substantial lactic acid leading to the pH decline in the microenvironment. In recent years, numerous studies have sought to identify new targets to inhibit *S. mutans* (Phan & Marquis, 2006; Bowen & Koo, 2011; Zhang *et al*., 2015). For instance, Zhang *et al.* have screened out several novel small molecules targeting dihydrofolate reductase that could inhibit the biofilm formation of *S. mutans*. Genes encoding Alr (*smu.1834*) and Ddl (*smu.599*) were found in the genome of *S. mutans* UA159 (Ajdic *et al*., 2002). It is plausible that these two enzymes, which are involved in D-Ala metabolism, could be potential antimicrobial targets in *S. mutans*.

Before searching for drugs specifically targeting the D-Ala metabolism in *S. mutans*, we needed to first confirm the physiological functions of this metabolic pathway in *S. mutans.* In this study, we found that pharmacological impairment of D-Ala metabolism by addition of DCS exhibited suppressive effects against the planktonic growth and biofilm formation of *S. mutans*, which could be rescued by the addition of D-Ala, indicating the indispensable functions of D-Ala metabolism in *S. mutans*.

METHODS

Bacterial strains and growth media

Streptococcus mutans UA159 was obtained from the American Type Culture Collection (Manassas, VA). *Streptococcus mutans* was routinely grown at 37° under aerobic condition (5% CO_2) in brain–heart infusion broth (BHI; Difco, Sparks, MD) or on BHI solid plate (BHI with 2% agar; Biotopped, Japan, Beijing, China). When needed, the medium was supplemented with 1% sucrose (designated BHIS), certain concentrations of DCS (Sigma, St Louis, MO), or D-Ala (Sigma), as detailed below.

Planktonic growth and biofilm analysis

The minimum inhibitory concentration (MIC) of DCS against *S. mutans* was determined as previously described (Fischer *et al*., 2013). Either 100 ppm or 150 ppm of DCS was used in the following experiments based on data obtained from the MIC assay. The potential inhibitory/reversible effects of DCS and D-Ala on the planktonic growth of *S. mutans* were monitored by measurement of the optical density of the cell culture at 600 nm.

The effects of DCS and D-Ala on biofilm formation by *S. mutans* were determined by crystal violet (CV) staining as described previously (Xu *et al*., 2011; Li *et al*., 2013; see Supplementary material, Appendix S1 and Table S1, for details). Each well of a 96-well microtiter plate containing 50% BHIS was inoculated with an overnight culture of *S. mutans* [1×10^6 colony-forming units (CFU) ml^{-1}], along with differing concentrations of DCS and D-Ala. The images of CV-stained 24-h biofilms were captured by an EZ4-HD stereomicroscope (Leica, Wetzlar, Germany), and representative pictures are shown.

The architecture of *S. mutans* biofilms was examined by scanning electron microscopy (FEI, Hillsboro, OR). Each well of a 24-well plate contained a saliva-coated glass coverslide and 50% BHIS was inoculated with an overnight culture of *S. mutans* (1×10^6 CFU ml^{-1}), and differing concentrations of DCS and D-Ala. After 24 h of incubation, biofilms were fixed with glutaraldehyde at room temperature for 12 h, then serially dehydrated in ethanol, and sputter-coated with gold. Specimens were examined at ×2000 and ×5000 magnifications, and representative pictures are shown.

The effect of DCS on the preformed biofilms of *S. mutans* was determined by a standard plate count method as described previously (Li *et al*., 2014). A 200-μl quantity of *S. mutans* UA159 cell suspension (1×10^6 CFU ml^{-1}) in BHIS was added to the wells of a 96-well microtitre plate for biofilm formation. After anaerobic incubation at 37°C for 24 h, the growth medium was removed without disrupting the integrity of the biofilms. The formed biofilms were then washed three times with phosphate-buffered saline (PBS, pH 7.2) to remove non-adherent cells. Then, 50% BHIS supplemented with different concentrations of DCS (75–2400 ppm) was added to wells containing biofilm and incubated at 37°C for 24 h. The control wells contained 50% BHIS without DCS. After incubation, the culture media were removed, and the treated biofilms were washed three times with PBS (pH 7.2). Then the biofilm cells were suspended

in saline [0.9%, weight/volume (w/v)] and sonicated for 45 s to separate cells using an ultrasonifier (output control at 8, and Duty cycle of 70; Branson Sonifier 450; Fisher Scientific, Pittsburgh, PA) for two separate cycles, with 2 min on ice between treatments. To determine the number of viable bacterial cells (in CFU), the dispersed biofilm cells were diluted $1 : 10^5$ and plated on BHI solid plates. The plates were anaerobically incubated at 37°C for 48 h, and the colonies were counted using an automated colony counter. The data were reported as log CFU ml^{-1}.

Biofilm viability analysis

Overnight cultures of *S. mutans* were inoculated on saliva-coated glass coverslips (1×10^6 CFU ml^{-1}). Different concentrations of DCS and D-Ala, in 2 ml of 50% BHIS media were then added to each culture well. Biofilms were stained after 24 h of growth using the BacLight live/dead kit (Molecular Probes, Eugene, OR; Zhou *et al.*, 2014). Live bacteria were stained with SYTO 9 whereas bacteria with compromised membranes were stained with propidium iodide. Biofilm images were captured using a Leica DMIRE2 confocal laser scanning microscope (CLSM; Leica) equipped with a 63× (1.4 numerical aperture) oil immersion objective lens. The image collection gates were set to 495–515 nm for SYTO 9, and 655–690 nm for propidium iodide. The detector gain (=500 V) and offset (=0%) were kept constant during image capture. Each biofilm was scanned at five randomly selected positions. Three-dimensional images of biofilms were rendered by IMARIS 7.0 software (Bitplane, Zurich, Switzerland), and representative pictures are shown. The biofilm biomass (μm^3 μm^{-2}) of each channel was calculated by COMSTAT (Heydorn *et al.*, 2000; Xiao *et al.*, 2012).

Transmission electron microscopy

Transmission electron microscopy was used to investigate the effects of DCS and D-Ala on the cell wall of *S. mutans* in planktonic cultures. Overnight cultures of *S. mutans* were inoculated into 50% BHI media with differing concentrations of DCS and D-Ala. After incubation, the mid-log phase bacteria (optical density of the cell culture at 600 nm ~0.5) were collected by centrifugation at 4000 ***g*** for 10 min. The pellets were washed twice in 200 mM sodium cacodylate buffer, pre-fixed in 2.5% (w/v) glutaraldehyde and fixed with 1% (w/v) OsO_4. The samples were embedded in Epon resin and thin sections (60 nm) were prepared using a microtome. Sections were stained with 4% (w/v) uranyl acetate and then with 0.4% (w/v) lead citrate, and examined with a Tecnai G^2 F20 S-TWIN electron microscope (FEI).

Atomic force microscopy

The atomic force microscopy (AFM) assay was performed as described by Sharma *et al.* (2014) with some modifications. Adhesion force measurements were conducted using a SHIMADZU STM9700 system (Shimadzu Corp., Kyoto, Japan), in the contact mode using a tipless cantilever (Shimadzu Corp.). In brief, each well of a 24-well plate contained a slice of saliva-coated glass coverslide and 50% BHIS was inoculated with an overnight culture of *S. mutans* (1×10^6 CFU ml^{-1}), and differing concentrations of DCS and D-Ala. After overnight *S. mutans* biofilm formation, the plates were rinsed with PBS (pH 7.2) three times to remove planktonic and loosely bound cells. Biofilm adhesion was measured using AFM under PBS, pH 7.2 at room temperature (20°C). A total of 100 force–distance curves were obtained at 10 different *S. mutans* biofilm regions for each group, at a scan rate of 0.5 Hz, ramp size of 18 μm, and with a trigger force of 5 nN (see Supplementary material, Appendix S2, for details). Adhesion forces were calculated from force–distance curves using built-in software within the STM9700 system. The data are reported as the median and interquartile ranges, with the data distribution also plotted.

Bacteria/extracellular polysaccharides staining

Overnight cultures of *S. mutans* (1×10^6 CFU ml^{-1}) were inoculated on saliva-coated glass coverslips in 2 ml of 50% BHIS media containing different concentrations of DCS and D-Ala. The bacteria and extracellular polysaccharides (EPS) of 24-h biofilms were double-labeled with fluorescent probes as previously described (Xiao *et al.*, 2012; Zheng *et al.*, 2013, 2015; see Supplementary material, Appendix S3, for details). Images of five random fields of each group were captured using a Leica DMIRE2 CLSM (Leica) and representative pictures are shown. The EPS/bacteria ratio was calculated with COMSTAT software.

Statistical analyses

All experiments were performed in triplicate with at least three biological replicates. Statistical analysis of the data was performed with SPSS software (version 16.0 for Windows; SPSS Inc., Chicago, IL) using one-way analysis of variance to compare the means of all groups and followed by Student–Newman–Keuls test to compare the means of each of the two groups. AFM data were analyzed by the Wilcoxon test. Data were considered significantly different if the two-tailed P value was <0.05.

RESULTS

DCS inhibited planktonic growth and biofilm formation of *S. mutans*

As an irreversible inhibitor against D-Ala metabolism, DCS exhibited a suppressive effect on the planktonic growth of *S. mutans* (Fig. 1A). The MIC of DCS against *S. mutans* was 150 ppm, whereas 100 ppm DCS already showed a remarkable antimicrobial effect. Of note, exogenous D-Ala could rescue the antimicrobial effects of DCS towards *S. mutans*. To completely compensate for the inhibitory effects of 100 ppm DCS, 150 ppm D-Ala was required (Fig. 1A).

Analysis of biofilm formation using the CV staining assay revealed that DCS and D-Ala had similar effects on *S. mutans* biofilm formation to those that they had on planktonic growth (Fig. 1B). Meanwhile, higher concentrations of DCS treatment of pre-formed *S. mutans* biofilms could induce a biofilm reduction as well (Fig. 1C). We then performed a scanning electron microscopy assay to investigate the architecture of the *S. mutans* biofilms at 24 h, which confirmed the results of CV staining (Fig. 1D). When DCS was added to the cultures, the biofilm volume decreased significantly compared with the control group. Moreover, we found a mass of heteromorphic micro-colonies in the biofilm images within the '150-ppm DCS' group (yellow arrows in Fig. 1D).

DCS affected *S. mutans* cell integrity

To investigate bacterial viability in *S. mutans* biofilms under the effect of DCS or D-Ala, live/dead staining assay was performed. Typical CLSM 3-D images of 24-h *S. mutans* biofilms are shown in Fig. 2A, where live bacteria were stained green and dead bacteria were stained red. Meanwhile, quantitative analysis was performed to determine the total biomass and the ratio of live/dead bacteria (Fig. 2B). The data confirmed that DCS could suppress the total biomass of *S. mutans* biofilm. Moreover, the live/dead bacterial ratios of the biofilms in '100-ppm DCS' and '150-ppm DCS' groups were significantly lower than that in control group. Meanwhile, the biofilms in the '100-ppm DCS + 150-ppm D-Ala' group exhibited total biomass and live/dead cell ratio similar to those of the control group.

The morphology of the *S. mutans* cells was examined by transmission electron microscopy (Fig. 2C). We found that damaged cells were present (red arrows in Fig. 2C) in the '100-ppm DCS' and '150-ppm DCS' groups. Compared with intact cells (green arrows in Fig. 2C), it appeared that the damaged cells displayed cell wall damage.

DCS compromised the ability of *S. mutans* to adhere to surfaces

The adhesion force of a certain site in *S. mutans* biofilm could be calculated from force–distance curves obtained by AFM. To investigate the effects of DCS and D-Ala on the adhesion ability of *S. mutans*, 10 randomly chosen sites per sample (each group has three samples) were analyzed. Quantitative data are summarized in Fig. 3. The adhesion forces of *S. mutans* biofilm in DCS-treated groups were significantly lower compared with the control group, whereas the '100-ppm DCS + 150-ppm D-Ala' group showed no significant difference to the control group.

The EPS matrix is of vital importance to the ability of *S. mutans* to adhere. We performed a bacteria/EPS staining assay to determine whether DCS and D-Ala could influence EPS production, so affecting the adhesion of *S. mutans* biofilms. Representative images of bacteria/EPS staining of *S. mutans* biofilms are shown in Fig. 4A, and the EPS/bacteria ratio was calculated as an indicator of EPS production (Fig. 4B). The data showed that the addition of DCS could dramatically restrain EPS production, whereas the addition of D-Ala could restore EPS/bacteria ratio to a normal level (control group).

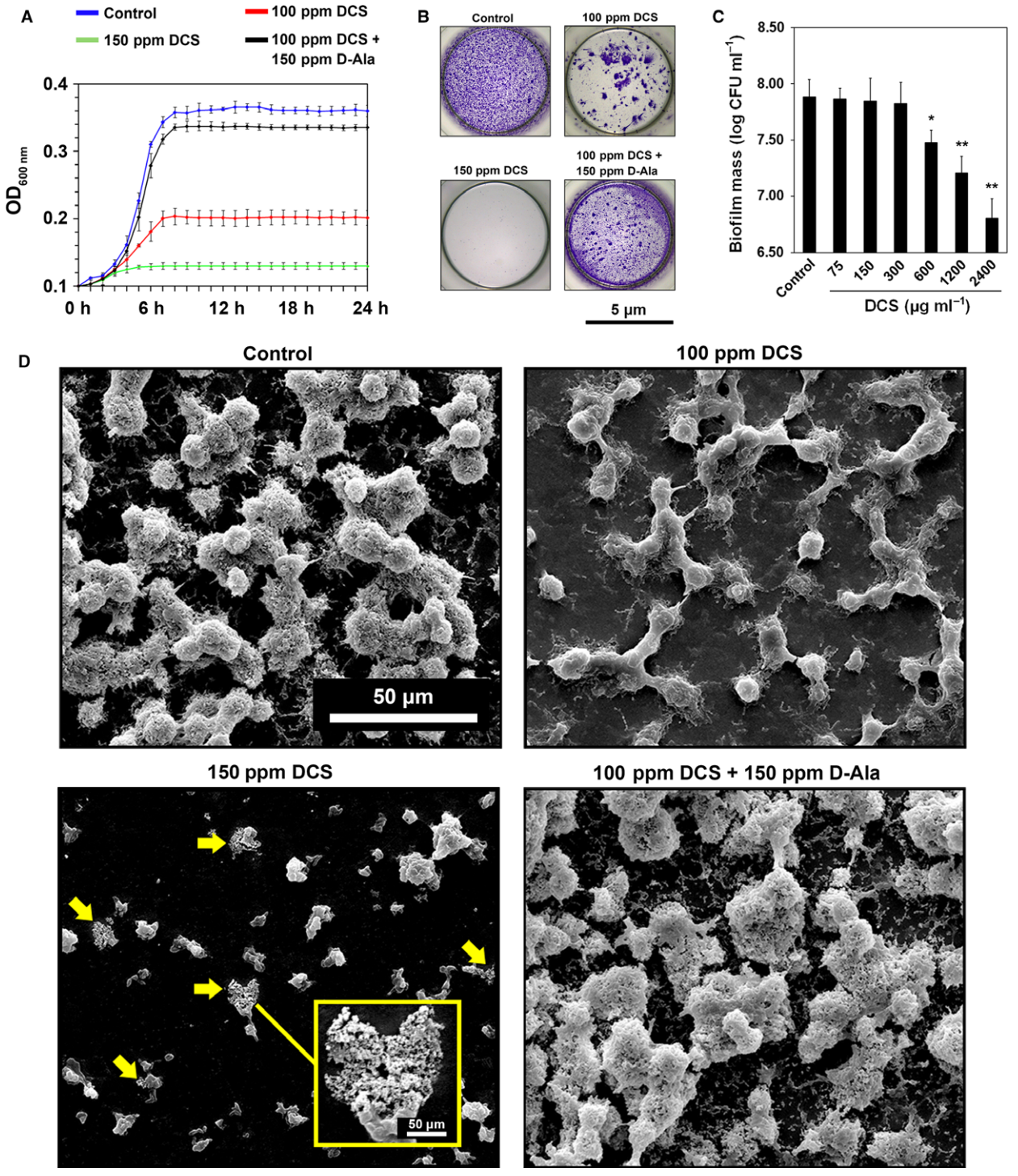

Figure 1 (A) Growth curves of *Strpetococcus mutans* in planktonic cultures, and each experiment was repeated at least three times. (B) Stereomicroscopy images of 24-h *S. mutans* biofilms stained with crystal violet, the scale line means magnification of the 96-well template. (C) The biomass of *S. mutans* biofilm under the effect of different concentrations of D-cycloserine (DCS). *Significant difference compared with non-treated controls ($P < 0.05$), **Significant difference compared with non-treated controls ($P < 0.001$). (D) Scanning electron microscopy images of 24-h *S. mutans* biofilms. The yellow arrows indicate a mass of heteromorphic micro-colonies, especially shown in the yellow box. Representative images are shown from at least five randomly selected positions of each sample.

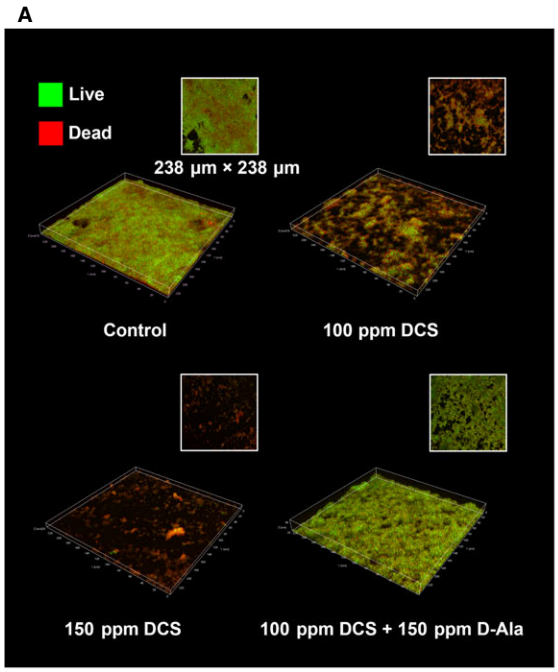

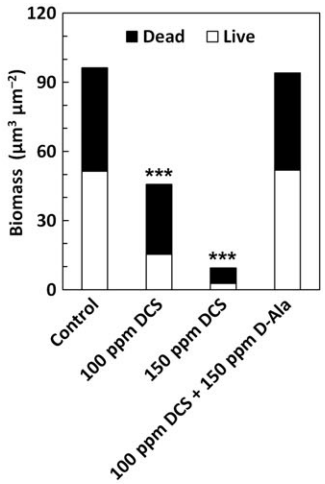

	Control	100 ppm DCS	150 ppm DCS	100 ppm DCS + 150 ppm D-Ala
Live/dead ratio	1.15 ± 0.05	0.48 ± 0.14***	0.40 ± 0.11***	1.23 ± 0.07

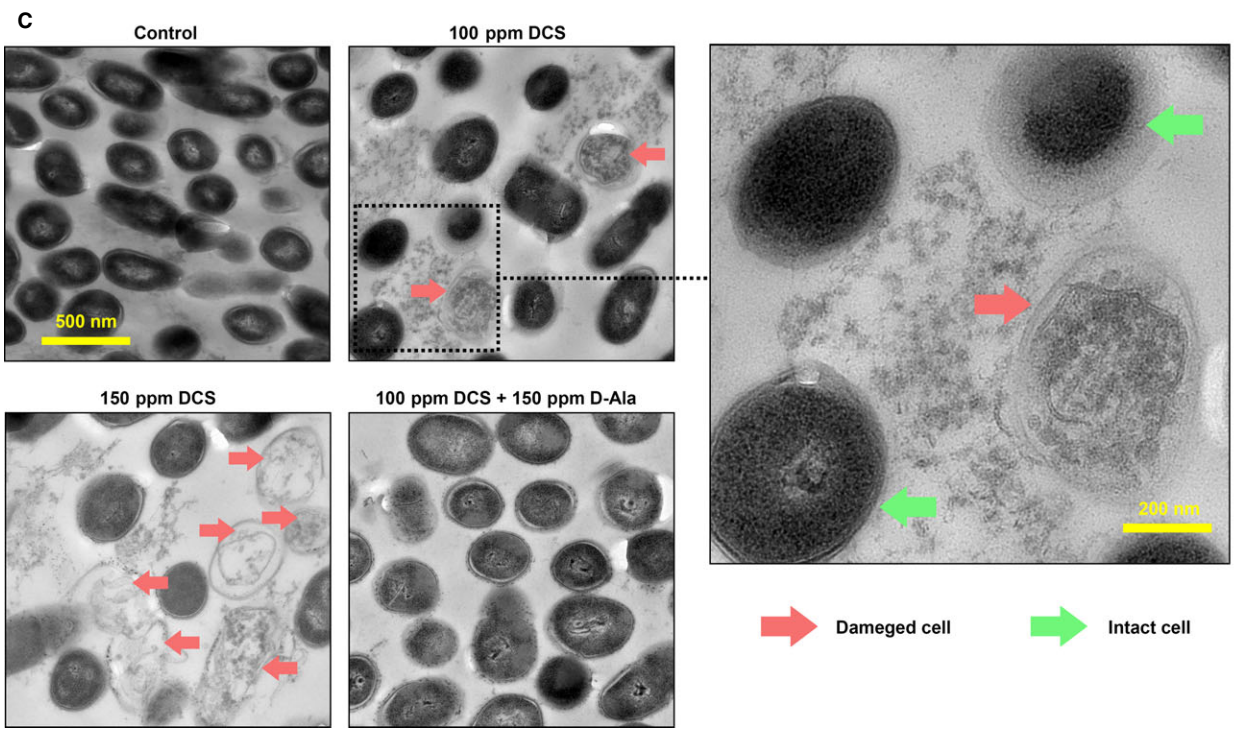

Figure 2 (A) Typical confocal laser scanning microscope three-dimensional images of 24-h biofilms of *Streptococcus mutans* stained with SYTO 9 (green, live bacteria) and propidium iodide (red, dead bacteria). (B) Quantitative analysis of live and (or) dead bacterial biomass performed with COMSTAT. Results are averaged from five randomly selected positions of each sample and presented as mean ± standard deviation. ***Significant difference compared with non-treated controls ($P < 0.0001$). (C) Transmission electron microscopy images of planktonic cells of *S. mutans*. Green arrows indicate intact cells, and red ones indicate damaged cells. Representative images are shown from at least five randomly selected positions of each sample.

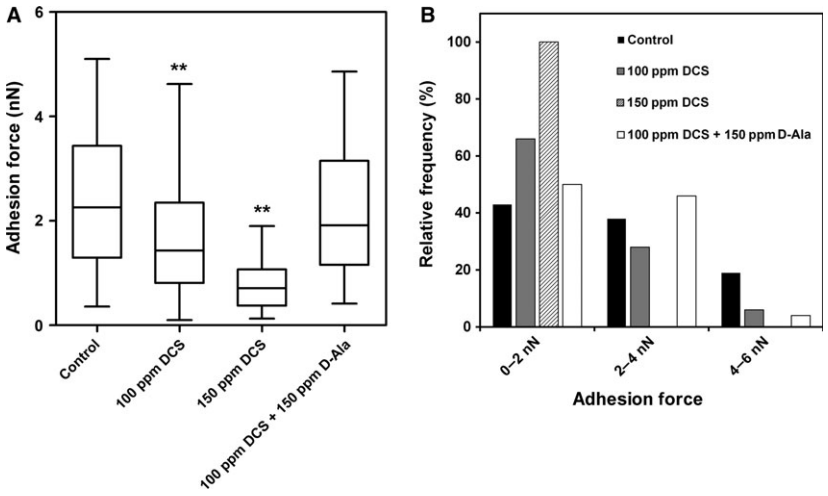

Figure 3 Atomic force microscopy (AFM) analysis of 24-h *S. mutans* biofilms. Adhesion force was measured by a SHIMADZU STM9700 system. (A) Data of the adhesion forces showed as the median and interquartile range. (B) The distribution characteristics of the adhesion forces. The data presented here are representative of three independent experiments. All AFM measurements were obtained under phosphate-buffered saline (pH 7.2). **Significant difference compared with non-treated controls ($P < 0.001$).

DISCUSSION

Enzymes involved in D-Ala metabolism provide attractive targets for the development of antimicrobial drugs (Watanabe *et al*., 2002; Prosser & de Carvalho, 2013) as they play a critical role in disease-causing bacteria, such as tuberculosis-causing mycobacteria (Sassetti *et al*., 2003). We have previously found that the growth of *alr*$^{-/-}$ *S. mutans* UA159 was restored when cultured in medium supplemented with D-Ala (data not shown). Halouska *et al.* (2014) found that the main lethal target of DCS in mycobacteria was the D-alanine–D-alanine ligase. This suggested that the D-alanine–D-alanine ligase gene of *S. mutans* UA159 might also be essential for cell survival, which therefore limits the use of gene knockouts to study the D-Ala metabolism. As such, we used DCS to inhibit D-Ala metabolism, allowing us to indirectly study the function of D-Ala metabolism in *S. mutans.* As a second-line anti-tuberculosis drug, DCS on the one hand irreversibly inhibits Alr and reduces D-Ala synthesis through competitive binding to the Alr coenzyme pyridoxal phosphate. On the other hand, DCS inhibits Ddl activity by competing with D-Ala for the substrate-binding site of Ddl, which reduces the number of precursors that participate in peptidoglycan biosynthesis. Meanwhile, exogenous D-Ala can bypass the L-Ala to D-Ala pathway and compete with DCS for the substrate-binding site of Ddl, restoring bacterial growth inhibited by DCS (Prosser & de Carvalho, 2013) .

When adding DCS to the medium, the planktonic growth of *S. mutans* was significantly inhibited. Consistent with our hypothesis, the addition of D-Ala was able to rescue the planktonic growth of *S. mutans* from the inhibitory effect of DCS. Moreover, the transmission electron microscopy results confirmed that the addition of DCS resulted in a cell wall defect in *S. mutans*, which could be restored by the addition of D-Ala. Here we have verified the indispensable function of D-Ala metabolism for the survival of *S. mutans* indirectly via the addition of DCS and/or D-Ala.

In addition, adding DCS significantly restrains the biofilm formation of *S. mutans*, which could be rescued by the addition of D-Ala. These results indicated that D-Ala metabolism played a critical role in biofilm formation in *S. mutans*, which is of paramount importance for the development of dental caries (Bhagwat *et al*., 2001). It is plausible that the impairment of D-Ala metabolism by the addition of DCS could induce a cell wall deficiency, which would be detrimental to the survival of *S. mutans* biofilm. To support this hypothesis, the live/dead staining assay results revealed that bacterial viability in DCS-treated biofilms was significantly lower.

As the ability of *S. mutans* to adhere to surfaces is essential for biofilm formation (Lee & Boran, 2003), we investigated whether D-Ala metabolism was involved in the adhesion process, and whether it could influence biofilm formation. The AFM assay determined the adhesion forces involved in *S. mutans* biofilms growing on saliva-coated glass coverslips and found that inhibition of D-Ala metabolism decreased the adhesion force. This phenomenon might be attributable to the role played by D-Ala in the formation of lipoteichoic acids (Milligan *et al*., 2007),

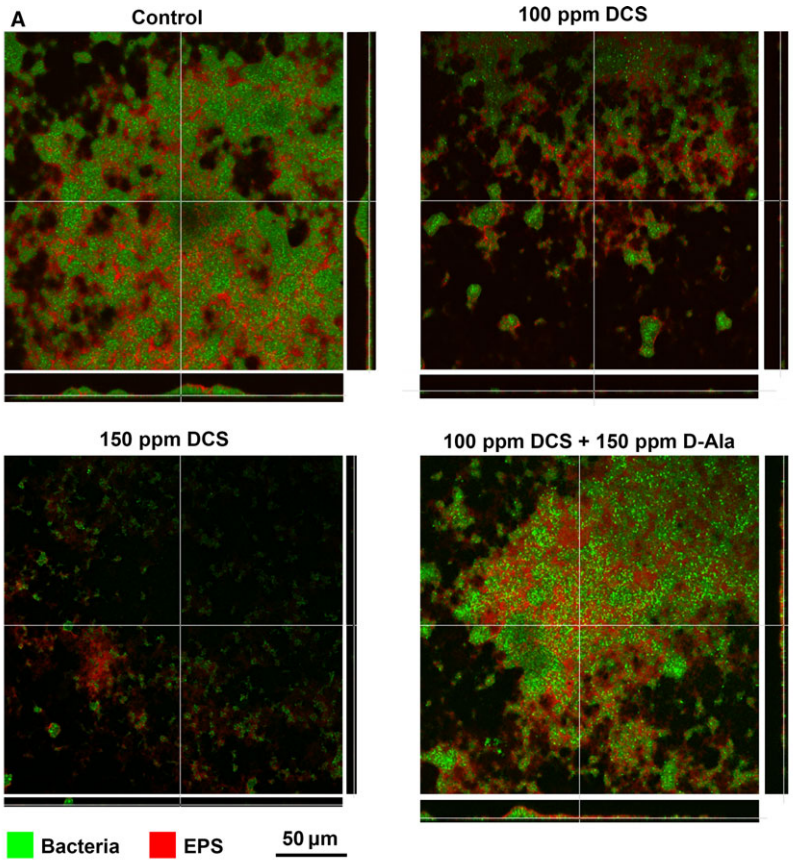

B

	Control	100 ppm DCS	150 ppm DCS	100 ppm DCS + 150 ppm D-Ala
EPS/bacteria ratio	1.10 ± 0.17	0.80 ± 0.11*	0.58 ± 0.19**	1.09 ± 0.10

Figure 4 (A) *Streptococcus mutans* 24-h biofilms stained with SYTO 9 (green, bacteria) and Alexa Fluor 647 labeled dextran (red, EPS). (B) Quantitative analysis of extracellular polysaccharide (EPS) biomass performed with COMSTAT. Results are averaged from five randomly selected positions of each sample and presented as mean ± standard deviation. ***Significant difference compared with non-treated controls ($P < 0.0001$).

which is closely associated with the sucrose-dependent adhesion process of *S. mutans* (Rolla *et al.*, 1980). It is noteworthy that the addition of DCS and/or D-Ala had an analogous effect on the EPS production, which is also of vital importance to sucrose-dependent adhesion in *S. mutans* (Koo *et al.*, 2010, 2013). Nevertheless, identifying the exact relationship between D-Ala metabolism and adhesion of *S. mutans* requires further studies.

Given the importance of D-Ala metabolism on the growth and biofilm formation of *S. mutans*, Alr and Ddl are potential new targets for anti-bacterial drugs. The oral cavity consists of a variety of microorganisms and to avoid non-specific inhibition of other bacteria by broad-spectrum antimicrobial drugs, the strategies for designing *S. mutans*-specific drugs proposed by the groups of Eckert and He (Eckert *et al.*, 2006; He *et al.*, 2010) can be used to design specific drugs that including killing, targeting and linker regions.

In conclusion, the current study provides the first evidence that D-Ala metabolism is essential for planktonic growth and biofilm formation of *S. mutans*. It would be possible to take Alr and/or Ddl of *S. mutans* as an antibacterial target to screen and optimize the safety and effective specificity of agents. In the future, we plan to design species-specific drugs targeting D-Ala metabolism, to counter the overgrowth of *S. mutans* under cariogenic conditions, which will contribute to the management of dental caries.

ACKNOWLEDGEMENTS

This study was supported by the National Natural Science Foundation of China (81400501 to ML and

81430011 to XZ); the International Science and Technology Cooperation Program of China 2014DFE30180 (XZ); and the Special Fund of the State Key Laboratory of Oral Diseases, Sichuan University (SKLOD201525 to ML). The authors declare no potential conflict of interest with respect to the authorship and/or publication of this article.

REFERENCES

Ajdic, D., McShan, W.M., McLaughlin, R.E. *et al.* (2002) Genome sequence of *Streptococcus mutans* UA159, a cariogenic dental pathogen. *Proc Natl Acad Sci USA* **99**: 14434–14439.

Batson, S., Rea, D., Fülöp, V. and Roper, D.I. (2010) Crystallization and preliminary X-ray analysis of D-alanyl-D-alanine ligase (EcDdlB) from *Escherichia coli*. *Acta Crystallogr Sect F Struct Biol Cryst Commun* **66**: 405–408.

Beighton, D. (2005) The complex oral microflora of high-risk individuals and groups and its role in the caries process. *Community Dent Oral Epidemiol* **33**: 248–255.

Bhagwat, S.P., Nary, J. and Burne, R.A. (2001) Effects of mutating putative two-component systems on biofilm formation by *Streptococcus mutans* UA159. *FEMS Microbiol Lett* **205**: 225–230.

Bowen, W.H. and Koo, H. (2011) Biology of *Streptococcus mutans*-derived glucosyltransferases: role in extracellular matrix formation of cariogenic biofilms. *Caries Res* **45**: 69–86.

Chacon, O., Bermudez, L.E., Zinniel, D.K. *et al.* (2009) Impairment of D-alanine biosynthesis in *Mycobacterium smegmatis* determines decreased intracellular survival in human macrophages. *Microbiology* **155**: 1440–1450.

Corby, P.M., Lyons-Weiler, J., Bretz, W.A. *et al.* (2005) Microbial risk indicators of early childhood caries. *Clin Microbiol* **43**: 5753–5759.

Eckert, R., He, J., Yarbrough, D.K., Qi, F., Anderson, M.H. and Shi, W. (2006) Targeted killing of *Streptococcus mutans* by a pheromone-guided "smart" antimicrobial peptide. *Antimicrob Agents Chemother* **50**: 3651–3657.

Fischer, C.L., Walters, K.S., Drake, D.R. *et al.* (2013) Oral mucosal lipids are antibacterial against *Porphyromonas gingivalis*, induce ultrastructural damage, and alter bacterial lipid and protein compositions. *Int J Oral Sci* **5**: 130–140.

Halouska, S., Fenton, R.J., Zinniel, D.K., Marshall, D.D., Barletta, R.G. and Powers, R. (2014) Metabolomics analysis identifies D-alanine-D-alanine ligase as the primary lethal target of D-cycloserine in *mycobacteria*. *J Proteome Res* **13**: 1065–1076.

He, J., Yarbrough, D.K., Kreth, J., Anderson, M.H., Shi, W. and Eckert, R. (2010) Systematic approach to optimizing specifically targeted antimicrobial peptides against *Streptococcus mutans*. *Antimicrob Agents Chemother* **54**: 2143–2151.

Heydorn, A., Nielsen, A.T., Hentzer, M. *et al.* (2000) Quantification of biofilm structures by the novel computer program COMSTAT. *Microbiology* **146**: 2395–2407.

Hols, P., Defrenne, C., Ferain, T., Derzelle, S., Delplace, B. and Delcour, J. (1997) The alanine racemase gene is essential for growth of *Lactobacillus plantarum*. *J Bacteriol* **179**: 3804–3807.

Koo, H., Xiao, J., Klein, M.I. and Jeon, J.G. (2010) Exopolysaccharides produced by *Streptococcus mutans* glucosyltransferases modulate the establishment of microcolonies within multispecies biofilms. *J Bacteriol* **192**: 3024–3032.

Koo, H., Falsetta, M.L. and Klein, M.I. (2013) The exopolysaccharide matrix: a virulence determinant of cariogenic biofilm. *J Dent Res* **92**: 1065–1073.

Lee, S.F. and Boran, T.L. (2003) Roles of sortase in surface expression of the major protein adhesin P1, saliva-induced aggregation and adherence, and cariogenicity of *Streptococcus mutans*. *Infect Immun* **71**: 676–681.

Li, M., Huang, R., Zhou, X. and Gregory, R.L. (2013) Role of sortase in *Streptococcus mutans* under the effect of nicotine. *Int J Oral Sci* **5**: 206–211.

Li, M., Huang, R., Zhou, X., Zhang, K., Zheng, X. and Gregory, R.L. (2014) Effect of nicotine on dual-species biofilms of *Streptococcus mutans* and *Streptococcus sanguinis*. *FEMS Microbiol Lett* **350**: 125–132.

Lu, Y.Z., Sheng, Y., Li, L.F. *et al.* (2007) Crystallization and preliminary crystallographic analysis of D-alanine-D-alanine ligase from *Streptococcus mutans*. *Acta Crystallogr Sect F Struct Biol Cryst Commun* **63**: 807–808.

Milligan, D.L., Tran, S.L., Strych, U., Cook, G.M. and Krause, K.L. (2007) The alanine racemase of *Mycobacterium smegmatis* is essential for growth in the absence of D-alanine. *J Bacteriol* **189**: 8381–8386.

Mullins, L.S., Zawadzke, L.E., Walsh, C.T. and Raushel, F.M. (1990) Kinetic evidence for the formation of D-alanyl phosphate in the mechanism of D-alanyl-D-alanine ligase. *J Biol Chem* **265**: 8993–8998.

Neuhaus, F.C. (1962) The enzymatic synthesis of D-alanyl-D-alanine. I. Purification and properties of D-alanyl-D-alanine synthetase. *J Biol Chem* **237**: 778–786.

Phan, T.N. and Marquis, R.E. (2006) Triclosan inhibition of membrane enzymes and glycolysis of *Streptococcus*

mutans in suspensions and biofilms. *Can J Microbiol* **52**: 977–983.

Prosser, G.A. and de Carvalho, L.P. (2013) Metabolomics reveal D-alanine:D-alanine ligase as the target of D-cycloserine in *Mycobacterium tuberculosis*. *ACS Med Chem Lett* **4**: 1233–1237.

Rolla, G., Oppermann, R.V., Bowen, W.H., Ciardi, J.E. and Knox, K.W. (1980) High amounts of lipoteichoic acid in sucrose-induced plaque in vivo. *Caries Res* **14**: 235–238.

Sassetti, C.M., Boyd, D.H. and Rubin, E.J. (2003) Genes required for mycobacterial growth defined by high density mutagenesis. *Mol Microbiol* **48**: 77–84.

Sharma, S., Lavender, S., Woo, J. *et al.* (2014) Nanoscale characterization of effect of L-arginine on *Streptococcus mutans* biofilm adhesion by atomic force microscopy. *Microbiology* **160**: 1466–1473.

Takahashi, N. and Nyvad, B. (2011) The role of bacteria in the caries process: ecological perspectives. *J Dent Res* **90**: 294–303.

Watanabe, A., Yoshimura, T., Mikami, B., Hayashi, H., Kagamiyama, H. and Esaki, N. (2002) Reaction mechanism of alanine racemase from *Bacillus stearothermophilus*: X-ray crystallographic studies of the enzyme bound with *N*-(5′-phosphopyridoxyl) alanine. *J Biol Chem* **277**: 19166–19172.

Xiao, J., Klein, M.I., Falsetta, M.L. *et al.* (2012) The exopolysaccharide matrix modulates the interaction between 3D architecture and virulence of a mixed-species oral biofilm. *PLoS Pathog* **8**: e1002623.

Xu, X., Zhou, X. and Wu, C.D. (2011) The tea catechin epigallocatechin gallate suppresses cariogenic virulence factors of *Streptococcus mutans*. *Antimicrob Agents Chemother* **55**: 1229–1236.

Zhang, Q., Nguyen, T., McMichael, M. *et al.* (2015) New small-molecule inhibitors of dihydrofolate reductase inhibit *Streptococcus mutans*. *Int J Antimicrob Agents* **46**: 174–182.

Zheng, X., Zhang, K., Zhou, X. *et al.* (2013) Involvement of gshAB in the interspecies competition within oral biofilm. *J Dent Res* **92**: 819–824.

Zheng, X., Cheng, X., Wang, L. *et al.* (2015) Combinatorial effects of arginine and fluoride on oral bacteria. *J Dent Res* **94**: 344–353.

Zhou, H., Weir, M.D., Antonucci, J.M., Schumacher, G.E., Zhou, X.D. and Xu, H.H. (2014) Evaluation of three-dimensional biofilms on antibacterial bonding agents containing novel quaternary ammonium methacrylates. *Int J Oral Sci* **6**: 77–86.

SUPPORTING INFORMATION

Additional supporting information may be found in the online version of this article at the publisher's web-site.